

Application of Linear Switched Reluctance Motor for Active Suspension System in Electric Vehicle

Zhang Zhu, Norbert C. Cheung and K.W.E Cheng

Department of Electric Engineering, The Hong Kong Polytechnic University, Hong Kong
E-mail: 09901316r@polyu.edu.hk

Abstract—Electromagnetic active suspension system is considered to have improved stability and better dynamic response, compared to the hydraulic active suspension system. This paper proposes an electromagnetic suspension system, comprising of a linear switched reluctance motor and a passive spring. The magnetic and electric characteristics of linear motor are studied using FEA method. The sprung mass acceleration and related force applied by the actuator are investigated under different road disturbance. Simulation results demonstrate that the proposed active suspension system has good dynamic response and better ride comfort.

Keywords— Active suspension system, Linear switched reluctance motor, Finite element

1. Introduction

The fundamental function of a vehicle suspension system is to maintain good contact between the wheels and the road surface, which is responsible for the holding capability and stability of the vehicle. Meanwhile, there exists another basic need for suspension system that related to ride quality. Human are susceptible to the discomforts of vibration and shocks induced by the road irregularities. However, the ride comfort and handling capability are considerably contradictory issues. It is difficult to achieve simultaneously a high performance of ride and handling under all driving conditions. The performance of conventional passive suspension systems is not satisfactory, since it is designed by considering a tradeoff between them.

In order to provide better dynamic characteristics, active suspension systems have been proposed and applied over the past decades, as the development of industrial technology and control method. Currently, two types of active suspension are mainly used: hydraulic and electromagnetic. Hydraulic suspension systems offer a higher force density, but also have a high system time constant. The limited bandwidth is proved to be insufficient for road irregularities with higher frequency. The shortcoming of hydraulic system is overcome by electromagnetic suspension systems with sufficient bandwidth actuator. Furthermore, the electromagnetic actuator can work in the generator mode and recover the energy back to the battery.[1] In general, the electromagnetic suspension systems can achieve better dynamic performance than any other suspension systems.

An electromagnetic suspension system comprises of an electromagnetic actuator and a mechanical spring. Several types of actuator have been presented by earlier researchers and companies. Linear brushless permanent magnet (LBPM) motor was proposed in [2, 3], and Bose Company applied a multi-phase alternating current (AC) electric motor in their suspension system. However, linear switched reluctance actuator (LSRA) has never been proposed to apply in active suspension systems. The LSRA has simple structure and free of permanent magnet, thus it is less expensive and more suitable for tough working environment.[4]

This paper is organized as follows. Section 2 presents the description of active suspension system, and analyzes the effect of system parameters. In section 3, a new tubular LSRA is proposed and the design is verified by FEA. In section 4, the control methodology of the whole system is studied, and performances are compared and evaluated by simulation. The conclusion is presented in section 5.

2. Suspension System Descriptions

In order to simplify the analysis of active suspension system, quarter car model is used, which is shown in Fig 1. Although the roll and pitch behaviors are eliminated, the fundamental performance of suspension system can be evaluated by adjusting the system parameters.

2.1 Passive Suspension System

Conventional passive suspension, as shown in Figure 1(a) consists of a linear spring that supporting the sprung mass and a damper dissipating the energy generated by the

movement. The tire is modeled as a spring of high stiffness that acting on both unsprung and sprung mass. The parameters of the quarter vehicle suspension are presented in Table 1.

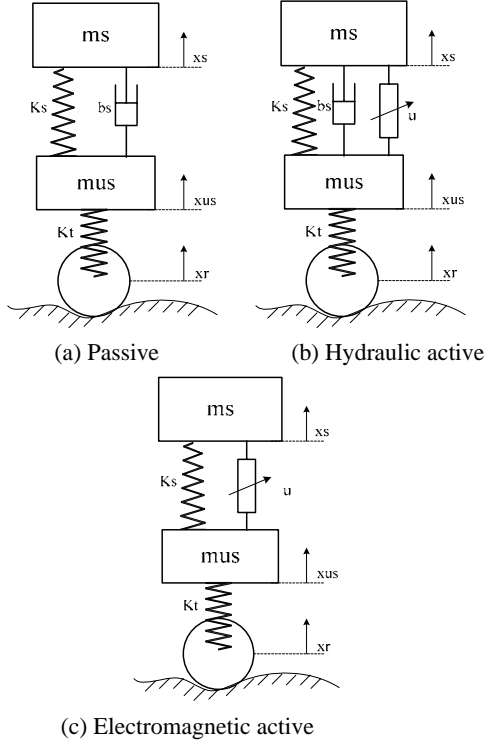


Figure 1: Quarter vehicle suspension model

The dynamic motion can be represented by the following equations:

$$m_s \ddot{x}_s + k_s (x_s - x_{us}) + b_s (\dot{x}_s - \dot{x}_{us}) = 0 \quad (1)$$

$$m_{us} \ddot{x}_{us} - k_s (x_s - x_{us}) - b_s (\dot{x}_s - \dot{x}_{us}) + k_t (x_{us} - x_r) = 0 \quad (2)$$

Where m_s and m_{us} are the sprung mass and unsprung mass, x_s and x_{us} are the displacements of respective masses, k_s and k_t are the spring stiffness, b_s is the damper coefficient and x_r represents the road disturbance.

2.2 Active Suspension System

The quarter model of hydraulic suspension system and the electromagnetic suspension system are shown in Figure 1(b) and (c), respectively. The hydraulic active suspension is passive suspension with an addition of

actuator between the sprung mass and unsprung mass. [5] The passive damper is replaced by an actuator in the electromagnetic suspension system.

Table 1: Suspension System Parameters

Parameter	Value
Sprung mass	400kg
Unsprung mass	50kg
Spring stiffness	20000N/m
Damper coefficient	1000N/m/s
Tire stiffness	180000N/m

The dynamic equations of active suspensions are:

$$m_s \ddot{x}_s + k_s (x_s - x_{us}) + b_s (\dot{x}_s - \dot{x}_{us}) = u \quad (3)$$

$$m_{us} \ddot{x}_{us} - k_s (x_s - x_{us}) - b_s (\dot{x}_s - \dot{x}_{us}) + k_t (x_{us} - x_r) = -u \quad (4)$$

Where u is the active force generated by actuator. The damping coefficient is set to zero when analyzing the electromagnetic suspension.

Considering the following state variables

$$x_1 = x_s - x_{us} \quad \text{Suspension deflection}$$

$$x_2 = \dot{x}_s \quad \text{Sprung mass velocity}$$

$$x_3 = x_{us} - x_r \quad \text{Tire deflection}$$

$$x_4 = \dot{x}_{us} \quad \text{Unsprung mass velocity}$$

We can obtain the state space equation

$$\dot{X} = AX + Bu + L\dot{x}_r \quad (5)$$

$$\text{Where } A = \begin{bmatrix} 0 & 1 & 0 & -1 \\ -\frac{k_s}{m_s} & -\frac{b_s}{m_s} & 0 & \frac{b_s}{m_s} \\ 0 & 0 & 0 & 1 \\ \frac{k_s}{m_{us}} & \frac{b_s}{m_{us}} & -\frac{k_t}{m_{us}} & -\frac{b_s}{m_{us}} \end{bmatrix}$$

$$B = \begin{bmatrix} 0 & \frac{1}{m_s} & 0 & -\frac{1}{m_{us}} \end{bmatrix}^T,$$

$$\text{and } L = \begin{bmatrix} 0 & 0 & -1 & 0 \end{bmatrix}^T$$

2.3 System Parameters Effect

From the dynamic equations, the open loop transfer functions are obtained. The effect of system parameters is investigated by looking at the bode plot.

The transfer function from road vertical velocity to sprung mass acceleration, suspension deflection and tire deflection are:

$$\frac{\ddot{x}_s}{\dot{x}_r} = \frac{k_t s(b_s s + k_s)}{d} \quad (6)$$

$$\frac{x_s - x_{us}}{\dot{x}_r} = -\frac{k_t m_s s}{d} \quad (7)$$

$$\frac{x_{us} - x_r}{\dot{x}_r} = -\frac{m_{us} m_s s^3 + (m_{us} + m_s) b_s s^2 + (m_{us} + m_s) k_s s}{d} \quad (8)$$

Where d is the system characteristic polynomial.

$$d = m_{us} m_s s^4 + (m_{us} + m_s) b_s s^3 + [(m_{us} + m_s) k_s + m_s k_t] s^2 + b_s k_t s + k_s k_t \quad (9)$$

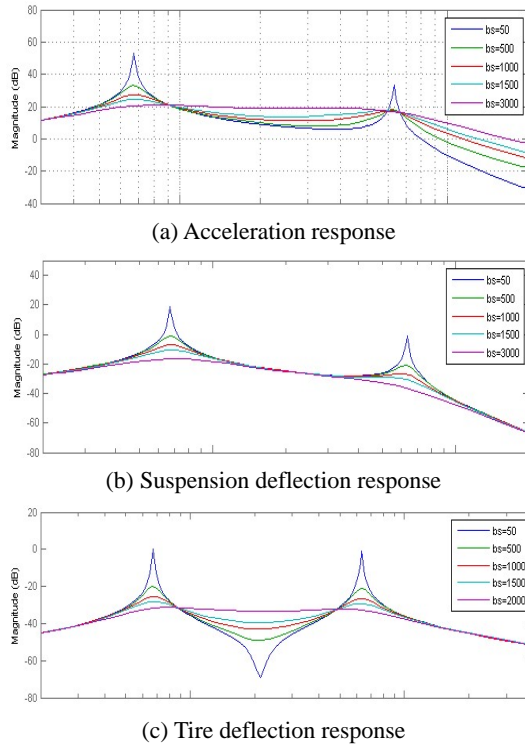


Figure 2: Effect of damping coefficient

In order to demonstrate the effect of damper, the resultant Bode plots for five damping coefficients are shown in Figure 2. In each plot, two peaks occur at the body natural frequency and wheel natural frequency. [6] It can be seen from the Figure 2(a), as the suspension damping coefficient decrease, the sprung mass acceleration response is deteriorated at low frequencies. The suspension deflection is improved obviously around

two natural frequencies with increased damping coefficient, as is shown in Figure 2(b). The effect on tire deflection is illustrated in Figure 2(c) that reduced tire deflection is obtained between the two natural frequencies with smaller damper, while the responses at two frequencies become worse.

The effect of spring stiffness is examined in Figure 3, by comparing five curves of increasing stiffness. The plot in Figure 3(a) shows the response of sprung mass acceleration. The isolation of vibration is increasingly improved as the spring stiffness is decreased. However, the suspension deflection at low frequencies is becoming severe, as shown in Figure 3(b) and (c).

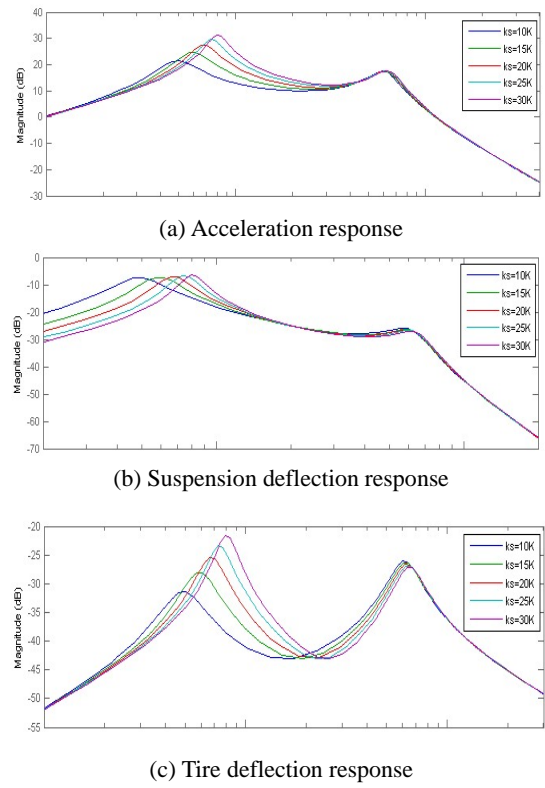


Figure 3: Effect of spring stiffness

3. Linear Switched Reluctance Actuator

3.1 System Specification

In order to design a linear switched reluctance actuator for suspension system, the suspension specification should be identified, according to the road irregularities and requirement by ride quality. Human will feel dizzy and seasick when subjected continuously to the acceleration between 0.5 and 1Hz. The sensitive frequency increases as the amplitude getting larger. Moreover, human body is also sensitive to frequencies from 18Hz to 20Hz. [7] The suspension displacement is

determined to have long enough stroke for coping with most road irregularities. The specification of suspension systems are listed in Table 2.

Table 2: Specification of Suspension System

<i>Specification</i>	<i>Value</i>
Maximum Force	4000N
Continuous Force	1000N
Maximum displacement	0.1m
Maximum speed	1m/s

3.2 Tubular LSRA Design

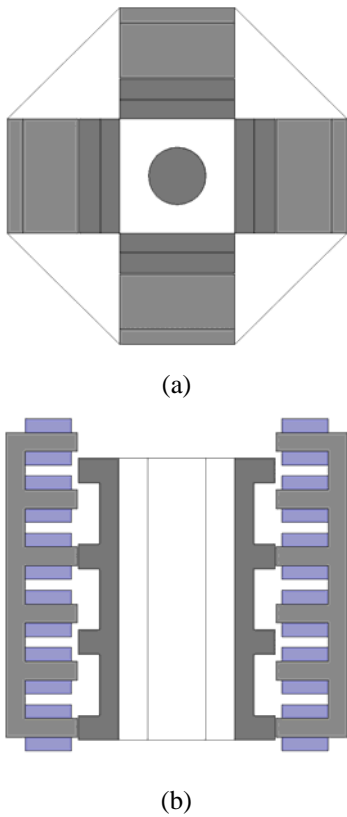


Figure 4: Configuration of TLSRA

The Tubular LSRA consists of four identical three-phase linear switched reluctance actuators, as shown in Figure 4. The stator and translator are laminated with silicon steel plates, and connected to the vehicle body and the wheel, respectively. In order to reduce the weight of translator, the phase windings are installed on the stator. Thus the translator is free of coils and permanent magnet that would not add too much weight on sprung mass. The windings of the same phase are connected in series. Only one converter is required, and it is relatively stationary to the stator. The mechanical parameters are listed in Table 3.

Table 3: TLSRA Parameters

<i>Specification</i>	<i>Value(mm)</i>
Stator pole width	16.667
Stator slot width	33.333
Translator pole width	27.667
Translator slot width	47.333
Yoke thickness	16.667
Stator pole height	45
Translator pole height	18
Stack length	80
Air-gap	0.8

3.3 Design Verification

To verify the design of TLSRA, two-dimensional finite element analysis (FEA) is used. Since the TLSRM is composed of four identical sections, the FEA can be simplified to analyze only one section. Figure 5 shows the flux linkage versus current at different translator positions between unaligned and aligned positions. The force profile at different currents and positions is shown in Figure 6. The position of 0mm represents the unaligned position, and the force reaches the largest value at an intermediate position.

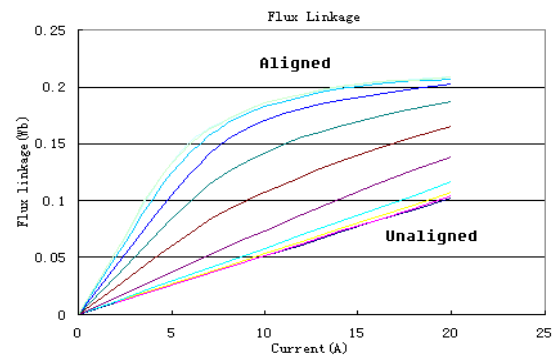


Figure 5: Flux linkage curves

Figure 7 shows the magnetic flux density distributions at position that generate largest force and the aligned positions. It can be seen from Figure 7(b) that there is severe local saturation in both pole corner in the low overlap position.

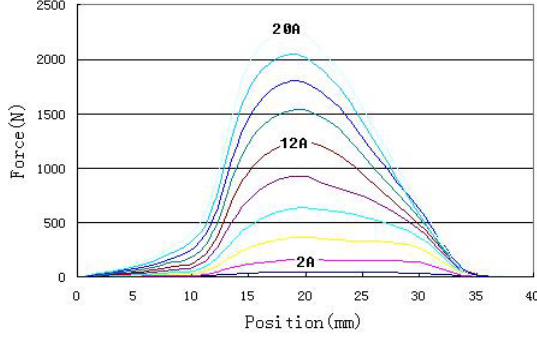
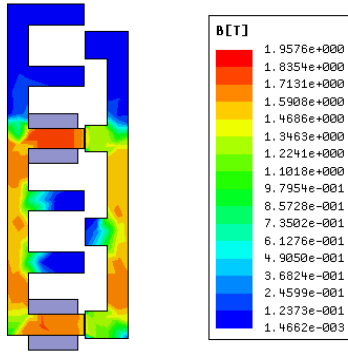
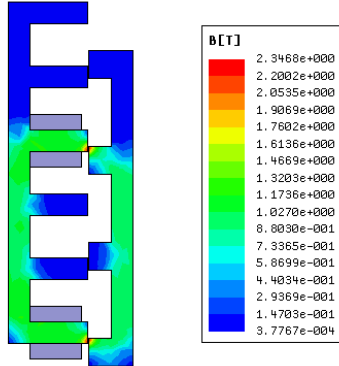


Figure 6: Force curves



(a)



(b)

Figure 7: Magnetic flux density

4. Controller Design and Simulation Results

In order to study the feasibility and evaluate the performance of the proposed suspension system, a control scheme is developed and simulated with the whole system. The control scheme has an outer loop to track the position reference of sprung mass and an inner loop to trace the required force for actuator. The controller block

diagram is shown in Figure 8. A LQR optimal controller is designed to obtain the required force. The LQR is a full state feedback controller with an aim to minimize a quadratic cost function. [8]

Considering the system state space model in equation (5), the quadratic cost function can be defined as:

$$\min J = \frac{1}{2} \int_0^{\infty} (x^T(t)Qx(t) + u^T(t)Ru(t))dt \quad (10)$$

Then the feedback control that minimizes the cost is

$$u = -KX \quad (11)$$

Where K is given by

$$K = R^{-1}B^T P(t) \quad (12)$$

And P is found by solving the continuous time Riccati differential equation

$$A^T P(t) + P(t)A - P(t)BR^{-1}B^T P(t) + Q = -\dot{P}(t) \quad (13)$$

Since the mechanical time constant is much bigger than that of electrical current, the electromagnetic variables can be considered as constant when the mechanical variables are mainly discussed. [9] The electromagnetic force of LSRA can be approximately described as

$$f_k(x, i_k) = \frac{1}{2} \frac{dL_k}{dx} i_k^2 \quad (14)$$

Where f_k is the electromagnetic force generated by phase k, dL_k/dx is the inductance change rate of phase k.

Based on this assumption, a winding excitation scheme for LSRA is followed to generate the active force. As shown in Figure 8, the scheme comprises a force distribution function (FDF) and force-current generation functions. The FDF is applied to calculate the reference force for each phase at specific position, and the force-current generation function that derived from equation (14) is used to obtain the phase current reference.

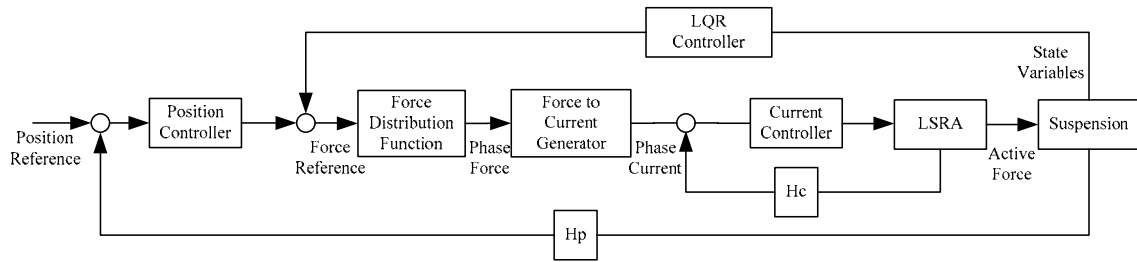
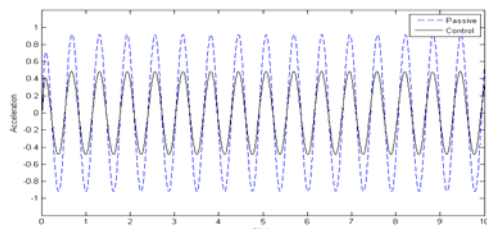
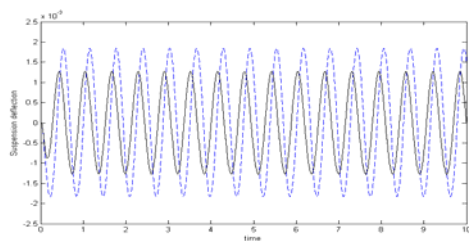


Figure 8: Controller block diagram

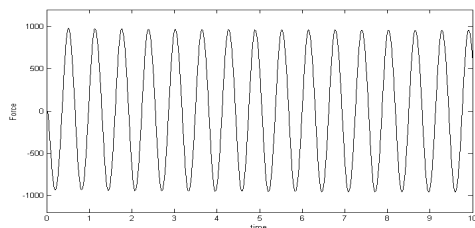
Simulations are performed in the Matlab/Simulink environment with the system parameters shown in Table I. Responses of sprung mass and suspension deflection at 10rad/second and 100rad/second sinuous disturbance are demonstrated in Figure 9 and Figure 10, respectively. The corresponding control forces are shown to illustrate the feasibility of the actuator. The sprung mass accelerations are improved significantly compared to the passive suspension. However, under the optimal control, the suspension deflection can not be reduced considerably at the same time. It becomes even worse than passive suspension at low frequency disturbance.



(a) Sprung mass acceleration



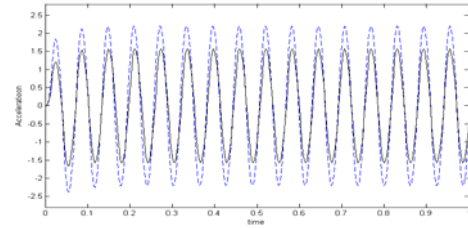
(b) Suspension deflection



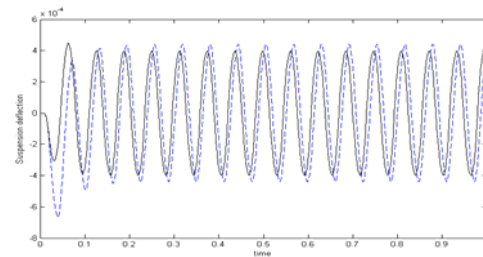
(c) Active force

Figure 9: System response at 10rad/s disturbance

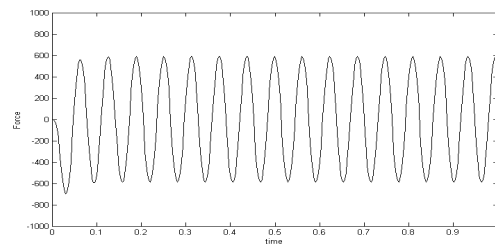
(Dashed line: passive, solid line: Active)



(a) Sprung mass acceleration



(b) Suspension deflection



(c) Active force

Figure 10: System response at 100rad/s disturbance

(Dashed line: passive, solid line: Active)

5. Conclusion

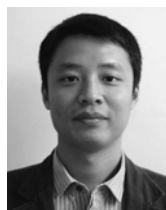
Improved ride quality and road holding capability are based on high performance suspension system. In this paper, the suspension parameters effects on system performance are examined, and we proposed an electromagnetic active suspension system that composed of linear switched reluctance actuator and mechanical spring. The design of LSRA is verified and optimized by FEA. Finally, the suspension system is simulated under the optimal control. Enhanced performance is achieved

by evaluating the response of sprung mass acceleration and suspension deflection.

6. References

- [1] B. L. J. Gysen, J. J. H. Paulides, J. L. G. Janssen and E. A. Lomonova, "Active Electromagnetic Suspension System for Improved Vehicle Dynamics," Vehicular Technology, IEEE Transactions on, vol. 59, pp. 1156-1163, 2010.
- [2] I. Martins, J. Esteves, G. D. Marques and F. Pina da Silva, "Permanent-magnets linear actuators applicability in automobile active suspensions," Vehicular Technology, IEEE Transactions on, vol. 55, pp. 86-94, 2006.
- [3] B. L. J. Gysen, J. L. G. Janssen, J. J. H. Paulides and E. A. Lomonova, "Design Aspects of an Active Electromagnetic Suspension System for Automotive Applications," Industry Applications, IEEE Transactions on, vol. 45, pp. 1589-1597, 2009.
- [4] K. Ramu, Switched Reluctance Motor Drives :Modeling, Simulation, Analysis, Design, and Applications. Boca Raton, FL: CRC Press, 2001.
- [5] R. Rajamani and J. K. Hedrick, "Adaptive observers for active automotive suspensions: theory and experiment," Control Systems Technology, IEEE Transactions on, vol. 3, pp. 86-93, 1995.
- [6] M. Appleyard and P. E. Wellstead, "Active suspensions: some background," Control Theory and Applications, IEE Proceedings -, vol. 142, pp. 123-128, 1995.
- [7] Donald Bastow and Geoffrey Howard, Car Suspension and Handling. London: Pentech Press, 1993.
- [8] M. Athans and P. L. Falb, Optimal Control :An Introduction to the Theory and its Applications. New York: Dover Publications, 2007.
- [9] Shi Wei Zhao, N. C. Cheung, Wai-Chuen Gan, Jin Ming Yang and Jian Fei Pan, "A Self-Tuning Regulator for the High-Precision Position Control of a Linear Switched Reluctance Motor," Industrial Electronics, IEEE Transactions on, vol. 54, pp. 2425-2434, 2007.

7. Author



Zhu Zhang

Department of Electric Engineering, The Hong Kong Polytechnic University

Tel: +852-67450964

He received the M.Eng, degree from South China University of Technology, Guangzhou,

China, in 2004. He is currently working toward the Ph.D. degree at the Department of Electric Engineering, The Hong Kong Polytechnic University, Kowloon, Hong Kong. His research interests include actuator design and power electronics.



Dr. N. C. Cheung (S'85–M'91–SM'05)

Department of Electric Engineering, The Hong Kong Polytechnic University

Tel: +852-27666182

He received the B.Sc. degree from the University of London, London, U.K., in 1981, the M.Sc. degree from the University of Hong Kong, Kowloon, Hong Kong, in 1987, and the Ph.D. degree from the University of New South Wales, Kensington, NSW, Australia, in 1996.

He is currently working in the Department of Electrical Engineering, Hong Kong Polytechnic University, Kowloon, Hong Kong. His research interests are motion control, actuators design, and power electronic drives.



Professor K. W. E. Cheng (M'90–SM'06)

Department of Electric Engineering, The Hong Kong Polytechnic University

Tel: +852-27666162

He received the B.Sc. and Ph.D. degrees from the University of Bath, Bath, U.K., in 1987 and 1990, respectively. He is currently a Professor and the Director of the Power Electronics Research Centre. He is the author of over 250 published papers and seven books. His research interests include power electronics, motor drives, electromagnetic interference, electric vehicle, and energy saving.